

Revisiting the evidence linking Arctic amplification to extreme weather in midlatitudes

Elizabeth A. Barnes¹

Received 17 July 2013; revised 8 August 2013; accepted 14 August 2013.

[1] Previous studies have suggested that Arctic amplification has caused planetary-scale waves to elongate meridionally and slow down, resulting in more frequent blocking patterns and extreme weather. Here trends in the meridional extent of atmospheric waves over North America and the North Atlantic are investigated in three reanalyses, and it is demonstrated that previously reported positive trends are likely an artifact of the methodology. No significant decrease in planetary-scale wave phase speeds are found except in October–November–December, but this trend is sensitive to the analysis parameters. Moreover, the frequency of blocking occurrence exhibits no significant increase in any season in any of the three reanalyses, further supporting the lack of trends in wave speed and meridional extent. This work highlights that observed trends in midlatitude weather patterns are complex and likely not simply understood in terms of Arctic amplification alone. **Citation:** Barnes, E. A. (2013), Revisiting the evidence linking Arctic amplification to extreme weather in midlatitudes, *Geophys. Res. Lett.*, *40*, doi:10.1002/grl.50880.

1. Introduction

[2] Near-surface Arctic temperatures have been warming at an accelerated rate relative to the midlatitudes and tropics [Serreze *et al.*, 2009; Screen and Simmonds, 2010]. This “Arctic amplification,” namely, the differential warming of the pole relative to lower latitudes, may alter midlatitude weather patterns by influencing the meridional temperature gradient and static stability, which largely drive the weather systems. Recent studies have investigated whether Arctic amplification has increased the frequency of observed extreme weather events [Liu *et al.*, 2012; Francis and Vavrus, 2012]. Liu *et al.* [2012] suggest that recent Arctic sea ice loss (which may be linked to Arctic amplification through a positive feedback process; see Screen and Simmonds [2010] for details) has caused an increase in snowfall over the United States and Europe through an increase in the frequency of blocking events. These blocking patterns are slow-moving (or stationary) waves that can persist for days and up to weeks, often bringing extreme weather to nearby regions [e.g., Black *et al.*, 2004; Dole *et al.*, 2011]. Similarly, Francis and Vavrus [2012] (FV12

hereafter) suggest that atmospheric Rossby waves have elongated meridionally in recent decades due to Arctic amplification. They hypothesize that these elongated waves propagate more slowly and favor more extreme weather conditions. They speculate that as the earth continues to warm, Arctic amplification will increasingly influence the North Atlantic atmospheric circulation, potentially causing more extreme weather in association with the slower waves.

[3] Motivated by these previous studies linking Arctic amplification to increased slow-moving Atlantic weather patterns, we seek to answer the following three questions: (1) Have wave extents increased over the past 30 years? (2) Have the phase speeds of large-scale atmospheric waves decreased? (3) Has the frequency of blocking events increased?

2. Methods

[4] To address the questions outlined above, we analyze wave properties using three reanalyses. The analysis covers the time period 1980–2011, and we compare trends in the European Centre for Medium-Range Weather Forecasts’s Era-Interim reanalysis [Dee *et al.*, 2011], the National Centers for Environmental Prediction/National Center for Atmospheric Research (NCEP/NCAR) Reanalysis [Kalnay *et al.*, 1996], and NASA’s Modern-Era Retrospective Analysis for Research and Applications (MERRA) reanalysis [Rienecker *et al.*, 2011]. Specifically, we focus on daily mean 500 hPa geopotential height (Z500) but also present results using daily mean 250 hPa meridional wind (v_{250}) and monthly mean 500 hPa zonal wind (u_{500}). Linear interpolation is used to obtain smooth contours from the gridded data. Trends are calculated using linear least squares regression, and the trends significantly different from 0 are determined using a two-sided t test at 90% and 95% confidence. We focus on the region that includes much of North America and the Atlantic Ocean basin (AtlanticNA; 230°E–350°E; 30°N–70°N) and note that this region is similar to the region studied by FV12. Meridional geopotential height extents are calculated using two different metrics:

[5] 1. The first metric is denoted as “SeaMaxMin” (seasonal maximum and minimum) and is similar but not identical to the method of FV12 (to be discussed). We will demonstrate that this metric does not capture the meridional extent of individual waves but rather the seasonal meridional excursions of the isopleths. SeaMaxMin extents are calculated using the seasonal maximum and minimum latitudes reached by individual Z500 isopleths. Specifically, for each season s , at each longitude λ , we find the maximum latitude $\theta_{\max}(s, \lambda)$ and minimum latitude $\theta_{\min}(s, \lambda)$ obtained by a specific Z500 isopleth over that season. The meridional extent is then calculated as $\theta_{\max}(s, \lambda) - \theta_{\min}(s, \lambda)$. An example of

Additional supporting information may be found in the online version of this article.

¹Department of Atmospheric Science, Colorado State University, Fort Collins, Colorado, USA.

Corresponding author: E. A. Barnes, Department of Atmospheric Science, Colorado State University, Fort Collins, CO 80523, USA. (eabarnes@atmos.colostate.edu)

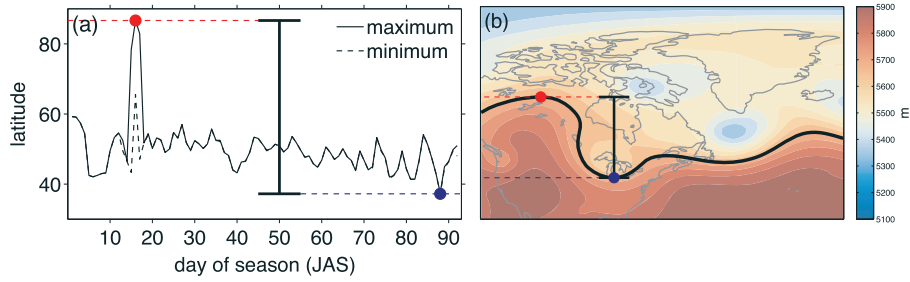


Figure 1. Examples of the (a) SeaMaxMin and (b) DayMaxMin meridional wave extent metrics for July–September 2009 (in Figure 1a) and 29 August 2009 (in Figure 1b) over the AtlanticNA region. In both panels the 5700 m Z500 isopleth is used and the vertical black bars denote the resulting meridional extent.

the metric calculation is shown in Figure 1a for $\lambda = 302^\circ\text{E}$ and $s = \text{July-August-September}$ in 2009. The solid black curve denotes the maximum latitude of the 5700 m isopleth each day of the season, and the dashed black curve similarly denotes the minimum latitude. The only way for the contour to have different maximum and minimum latitudes on a given day is by curling over (“breaking”), and this happens infrequently for this isopleth. Because of this, the seasonal maximum latitude (red dot) and minimum latitude (blue dot) nearly always occur on different days of the season (for the case in Figure 1a, days 16 and 88, 16 July and 26 September, respectively). Thus, the SeaMaxMin metric is a measure of the seasonal meridional excursion of the isopleth. We zonally average the extents over the AtlanticNA region to obtain an average for each season. FV12 did not zonally average

their data, and thus, SeaMaxMin is not identical to the metric presented in their study.

[6] 2. The second metric is called “DayMaxMin” and is designed to quantify the *daily* meanders of the Z500 field and, thus, the meridional extent of individual waves. For each day d , we calculate the maximum latitude $\theta_{\max}(d)$ and minimum latitude $\theta_{\min}(d)$ of a single Z500 isopleth over the AtlanticNA region, and the day’s meridional wave extent is calculated as $\theta_{\max}(d) - \theta_{\min}(d)$. Figure 1b shows an example of this calculation for 29 August 2009. The black contour denotes the 5700 m isopleth, and the black bar shows the distance between the maximum and minimum latitudes. Thus, this metric provides a single wave extent for every day of the season, and we average over the season to obtain an average wave extent.

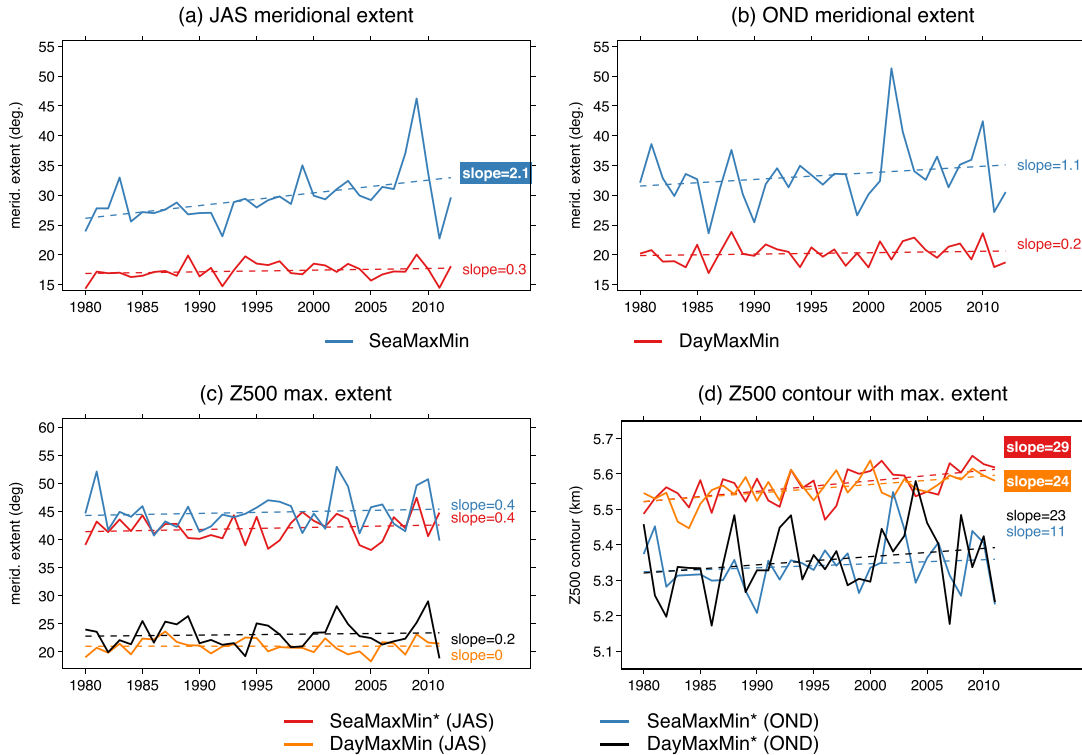


Figure 2. Two measures of observed AtlanticNA meridional geopotential isopleth extent as a function of time for (a) JAS and (b) OND from ERA-Interim. (c) The maximum meridional extent over a range of Z500 isopleths and (d) the Z500 isopleth with the maximum meridional extent. Dashed lines denote the linear least squares regression lines, with slopes given in degrees/decade (in Figures 2a–2c) and m/decade (in Figure 2d). Slopes statistically different from 0 at 90% (95%) confidence are enclosed in a white (colored) box.

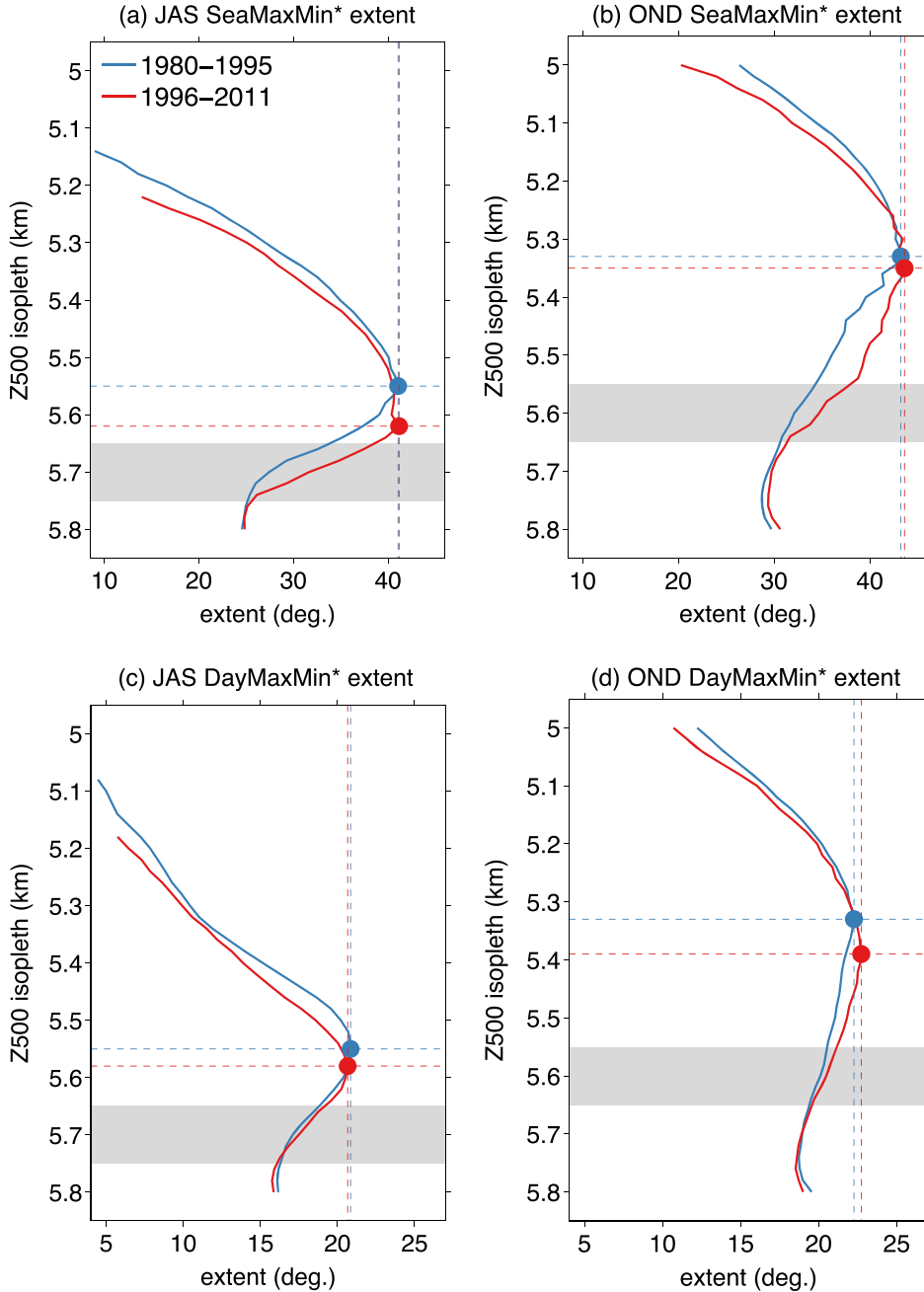


Figure 3. Seasonal AtlanticNA meridional extent as a function of Z500 isopleth and the method used: (a, b) SeaMaxMin* and (c, d) DayMaxMin* for JAS (Figures 3a and 3c) and OND (Figures 3b and 3d). Colored circles and dashed lines denote the maxima. Gray shading denotes the range of seasonal contours used in Figure 2.

[7] To follow the methods of FV12, both metrics are evaluated using three isopleths: [5650, 5700, 5750]m for July-August-September (JAS) and [5550, 5600, 5650]m for October-November-December (OND). Results are presented as the average meridional extent of the three isopleths. Finally, we focus first on the JAS and OND seasons since these are the two seasons with the largest trends found by FV12, although they also highlight trends in JFM.

[8] The phase speeds of the waves are diagnosed using Z500 and v250. We analyze the Z500 field to test the hypothesis that recent Arctic warming has caused waves on the Z500 field to slow down; however, we also include v250 to obtain an additional measure of wave propagation in

the upper troposphere, where Rossby wave phase speeds are often diagnosed, in order to evaluate the robustness of the trends [e.g., *Randel and Held, 1991; Chen and Held, 2007*]. The seasonal power spectra of the anomalous fields are calculated similarly to *Randel and Held [1991]*, and a detailed description of the methodology is provided in the supporting information. We are interested in planetary-scale Rossby waves and so limit the analysis to waves with zonal wave numbers 1–6 (results for wave numbers 1–3 are given in the supporting information). The phase speeds are area-weighted averaged between 30°N and 70°N to obtain a single phase speed over the region, but additional meridional bounds are reported in the supporting information and

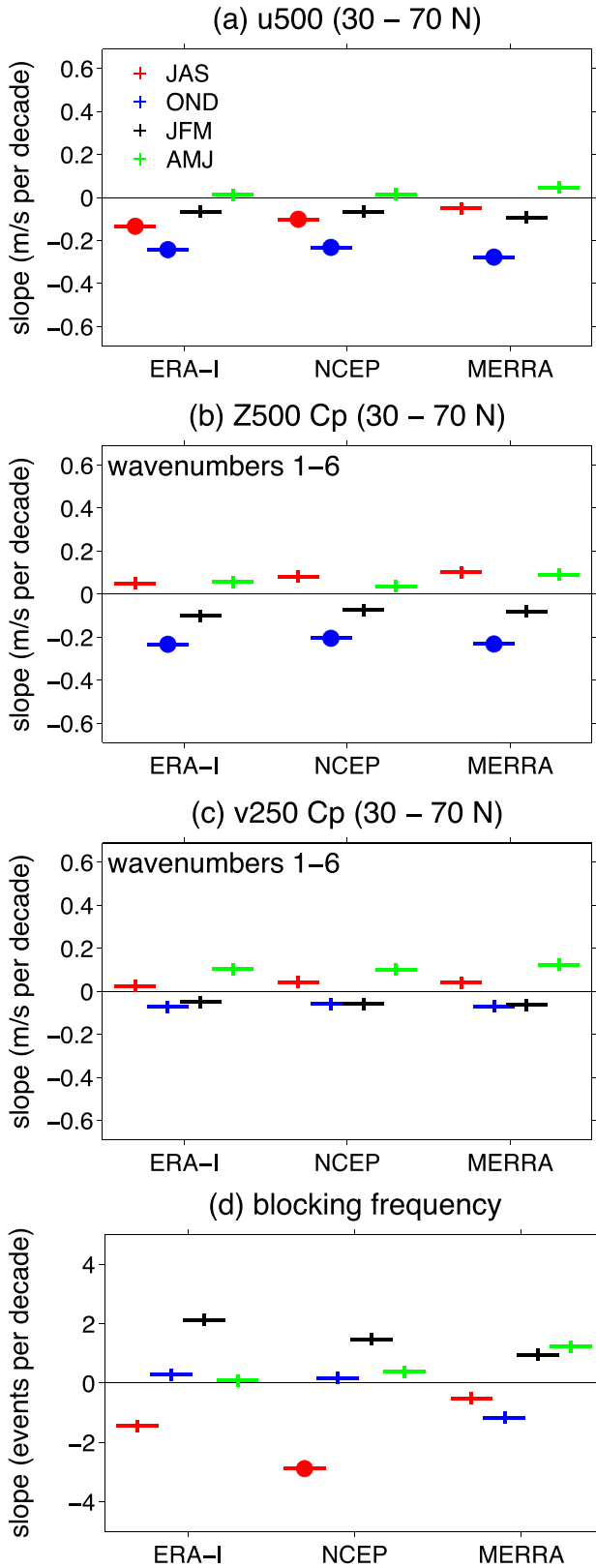


Figure 4. Seasonal trends of (a) u500, (b) Z500 phase speeds, (c) v250 phase speeds, and (d) blocking frequency. All trends are for the AtlanticNA region, and averages for Figures 4a–4c are taken between 30°N and 70°N. Phase speeds are for waves with zonal wave numbers 1–6. Open (closed) circles denote trends that are statistically different from 0 at 90% (95%) confidence.

discussed in the text. Finally, we directly address whether blocking events have increased in frequency by diagnosing blocking using the one-dimensional blocking algorithm of *Barnes et al.* [2012] which identifies blocking regimes when the Z500 field exhibits a persistent (5 days or longer) reversal of its gradient. A detailed description of the methodology is provided in the supporting information.

3. Results

[9] Figures 2a and 2b show time series of JAS and OND meridional extents calculated by the two metrics for ERA-Interim (results from NCEP and MERRA are similar). Beginning with the SeaMaxMin metric (blue curves), a significant trend emerges in JAS, with extents increasing over the past 30 years, while a large but nonsignificant trend is found in OND. Thus, the SeaMaxMin metric suggests that extents in JAS and OND have been increasing since 1980.

[10] If the SeaMaxMin metric captures the typical meridional extent of the large-scale propagating waves, then one would expect DayMaxMin to produce similar trends. Instead, very small, nonsignificant trends are seen in JAS and OND for DayMaxMin (red curves in Figures 2a and 2b). The meridional extents are smaller for DayMaxMin compared to SeaMaxMin because the extents of the isopleths in the SeaMaxMin method are not associated with any one wave as they are for DayMaxMin, but rather, the total seasonal extrema of an isopleth. Thus, trends calculated using the SeaMaxMin metric do not reflect trends in the properties of individual propagating waves. The observed wave extents, therefore, show no trend.

[11] We have demonstrated that trends in the meridional extent of waves are sensitive to the methodology. In addition, both SeaMaxMin and DayMaxMin suffer from another issue that leads to erroneous trends in wave meridional extents. We perform the same analysis but this time over a larger range of isopleths (5000–6000 m) and denote these metrics as SeaMaxMin* (Figures 3a and 3b) and DayMaxMin* (Figures 3c and 3d). The curves are separated into the beginning and end of the observational period to show changes in the wave extents. The y axis of Figure 3 specifies the isopleth, and the x axis denotes the meridional wave extent. The average latitude of each isopleth is provided in the supporting information.

[12] Beginning with Figures 3a and 3c, JAS meridional wave extents in 1980–1995 (blue curves) peak near 5550 m, signifying that this isopleth exhibits the largest meridional variations for both the seasonal (SeaMaxMin*) and daily (DayMaxMin*) metrics. In 1996–2011 (red curves), the isopleth with the maximum extent changes (variability moves to higher heights); however, the maximum wave extent does not change. Similar conclusions are drawn for OND (Figures 3b and 3d). In other words, the isopleth that is the most “wavy” increases, but the magnitude of the “waviness” remains the same. Why then did the SeaMaxMin and, to a lesser extent, DayMaxMin exhibit positive trends in wave extent? The reason lies in the original three isopleths analyzed, denoted as gray shading in Figure 3. For this narrow range of isopleths, the shift in the extent manifests itself as an increase in wave extents there; however, this increase is not robust across other isopleths.

[13] To further support this conclusion, Figure 2c displays the time series of the maximum extent of the waves

from Figure 3. No significant trends in the wave extents are found over any season for either SeaMaxMin* or DayMaxMin*. The Z500 isopleths that exhibit the maximum extent (Figure 2d) do, however, show significant positive trends. Thus, the trends in meridional wave extents over the past 30 years diagnosed in Figures 2a and 2b are likely largely due to the relocation of wave activity from one isopleth to another, with the wave extents themselves remaining relatively constant.

[14] This poleward shift of the Z500 isopleths is the manifestation of the high-latitude warming in the geopotential height field through the hypsometric equation. Note that the trends in the other metrics presented by FV12 (see their Figure 4), namely, the maximum latitude of an isopleth and the number of isopleth grid points north of 50°N, can also be explained by the poleward shift of the Z500 field, absent of any changes in the wave extents.

[15] FV12 suggest that Arctic warming may be reducing the zonal wind speeds over the Atlantic and that this reduction in the background flow may influence wave propagation speeds. Figure 4a shows trends in u500 area-weighted averaged between 30°N and 70°N for the three reanalyses. We choose to average over this range of latitudes in order to ensure that a meridional shift of the circulation will not appear as a decrease or increase in wind speed. Circled cross hairs denote significant trends, and all three reanalyses show a significant decrease in u500 during OND, as was documented in FV12. There is disagreement over the significance of the trend in JAS, and no significant trends are found in January-February-March or April-May-June.

[16] To determine whether the reduction in the background zonal flow has had a noticeable effect on wave propagation, Figure 4b shows the trends in the Z500 phase speeds. We find a robust decrease in wave phase speeds in OND, which is consistent with the u500 reductions. However, the phase speed trends are all positive for JAS although u500 is decreasing. Thus, the link between wave phase speed and u500 appears more complex than a simple one-to-one relationship. For comparison, Figure 4c shows phase speed trends calculated using v250, and no significant trend in wave phase speeds are found in any reanalysis in any season. We find that the degree to which the v250 and Z500 calculations agree is a strong function of the averaging domain, with both showing significant positive OND trends only when the speeds are averaged between 40°N and 60°N (see supporting information for additional averaging domains). Thus, we conclude that there is no robust observational evidence of decreasing wave speeds over the AtlanticNA region.

[17] Figure 4d shows the trends in blocking frequency over the AtlanticNA region. No statistically significant increase in blocking frequency is found, even in OND when the Z500 phase speeds have decreased. The lack of increasing trends in the atmospheric blocking patterns further supports the lack of trends in the wave meridional extents and wave phase speeds, and suggests that Arctic amplification over the past 30 years has not had a quantifiable impact on slow-moving weather patterns over North America or the North Atlantic.

4. Discussion and Conclusions

[18] We quantify observed trends in the meridional extent of waves over the North Atlantic/North America region

using two different metrics and three reanalyses. We find that the metrics disagree on whether a significant trend in wave extent has been observed, and we explain this disagreement as arising due to the methodology of defining the wave on either daily or seasonal time scales. In addition, we demonstrate that when both metrics focus on a narrow range of isopleths to track the ridges and troughs of a passing wave they incorrectly interpret a shift of the geopotential height field as a change in wave extent. When this shift is accounted for, no significant trend is found. We further investigate whether large-scale waves have slowed down in the recent decades and find no significant trends except in the Autumn months, although the significance of this trend is sensitive to the diagnostic field and the specific averaging domain. Furthermore, no significant increase in blocking occurrence is detected in any season. We conclude that the mechanism put forth by previous studies [e.g., Francis and Vavrus, 2012; Liu et al., 2012], that amplified polar warming has led to the increased occurrence of slow-moving weather patterns and blocking episodes, appears unsupported by the observations.

[19] A recent study by Screen and Simmonds [2013] also provides evidence that the trends in planetary waves suggested by FV12 may be an artifact of the methodology. They demonstrate that an alternative metric that is insensitive to a shift of Z500 does not yield significant positive trends in wave amplitude. The results presented here further suggest that the wave elongation reported by FV12 is at least partially an artifact of the poleward shift of the isopleths with polar warming.

[20] The Arctic is changing rapidly, and these changes will likely have profound effects on the Northern Hemisphere. This study, however, highlights that the relationship between Arctic amplification and midlatitude weather is complex. Additional influences from other latitudes, as well as internal variability [Screen et al., 2013], likely play an important role in determining the net atmospheric trends, and targeted modeling studies are needed to quantify the relative importance of polar changes on Atlantic weather.

[21] **Acknowledgments.** EAB thanks Isla Simpson and Lorenzo Polvani for their helpful comments on an earlier version of this manuscript and two anonymous reviewers for their constructive evaluations.

[22] The Editor thanks two anonymous reviewers for their assistance in evaluating this paper.

References

- Barnes, E. A., J. Slingo, and T. Woollings (2012), A methodology for the comparison of blocking climatologies across indices, models and climate scenarios, *Clim. Dynam.*, *38*, 2467–2481, doi:10.1007/s00382-011-1243-6.
- Black, E., M. Blackburn, G. Harrison, B. Hoskins, and J. Methven (2004), Factors contributing to the summer 2003 European heatwave, *Weather*, *17*, 4080–4088.
- Chen, G., and I. Held (2007), Phase speed spectra and the recent poleward shift of Southern Hemisphere surface westerlies, *Geophys. Res. Lett.*, *34*, L21805, doi:10.1029/2007GL031200.
- Dee, D. P., et al. (2011), The ERA-Interim reanalysis: Configuration and performance of the data assimilation system, *Q. J. R. Meteorolog. Soc.*, *137*(656), 553–597, doi:10.1002/qj.828.
- Dole, R., et al. (2011), Was there a basis for anticipating the 2010 Russian heat wave?, *Geophys. Res. Lett.*, *38*, L06702, doi:10.1029/2010GL046582.
- Francis, J. A., and S. J. Vavrus (2012), Evidence linking Arctic amplification to extreme weather in mid-latitudes, *Geophys. Res. Lett.*, *39*(6), L06801, doi:10.1029/2012GL051000.
- Kalnay, E., et al. (1996), The NCEP/NCAR 40-year reanalysis project, *Bull. Am. Meteorol. Soc.*, *77*, 437–471.
- Liu, J., J. Curry, and H. Wang (2012), Impact of declining Arctic sea ice on winter snowfall, *Proc. Natl. Acad. Sci. (USA)*, *109*(11), 4074–4079, doi:10.1073/pnas.1114910109.

BARNES: ARCTIC AMPLIFICATION AND WEATHER

- Randel, W., and I. Held (1991), Phase speed spectra of transient eddy fluxes and critical layer absorption, *J. Atmos. Sci.*, *48*, 688–697.
- Rienecker, M., et al. (2011), MERRA: NASA's Modern-Era Retrospective Analysis for Research and Applications, *J. Climate*, *24*, 3624–3648.
- Screen, J., C. Deser, I. Simmonds, and R. Tomas (2013), Atmospheric impacts of Arctic sea-ice loss, 1979–2009: Separating forced change from atmospheric internal variability, *Clim. Dynam.*, doi:10.1007/s00382-013-1830-9.
- Screen, J., and I. Simmonds (2013), Exploring links between Arctic amplification and midlatitude weather, *Geophys. Res. Lett.*, *40*, 1–6, doi:10.1002/GRL.50174.
- Screen, J. A., and I. Simmonds (2010), The central role of diminishing sea ice in recent Arctic temperature amplification, *Nature*, *464*(7293), 1334–7, doi:10.1038/nature09051.
- Serreze, M., A. Barrett, and J. Stroeve (2009), The emergence of surface-based Arctic amplification, *The Cryosphere*, *3*, 11–19.

SUPPLEMENTARY MATERIAL

Revisiting the evidence linking Arctic Amplification to extreme weather in mid-latitudes

Elizabeth A. Barnes¹

¹Department of Atmospheric Science, Colorado State University, Fort Collins, CO, USA.

Phase speed calculation

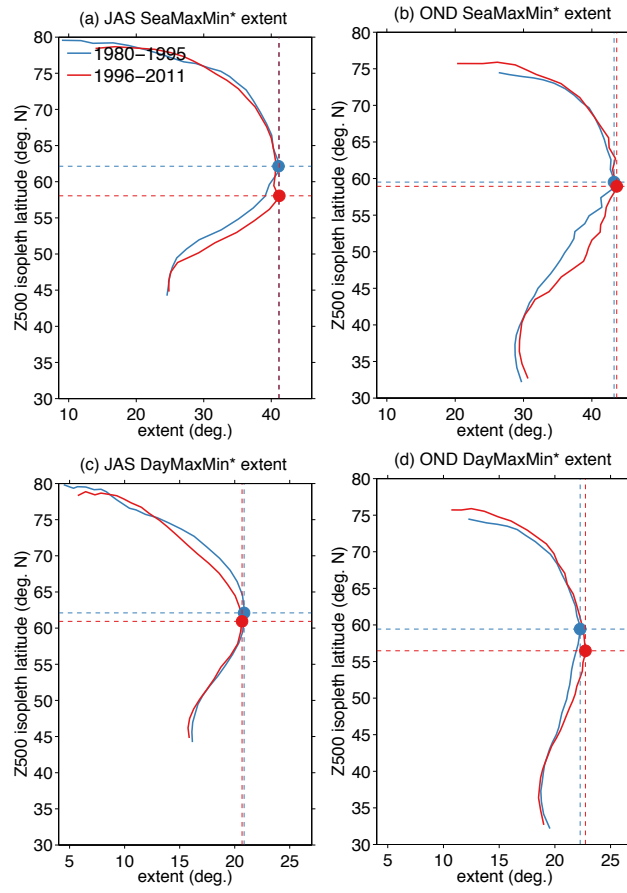
The seasonal power spectra of the anomalous fields are calculated similarly to [2], with anomalies defined as the deviations from the climatological mean plus the first four Fourier harmonics of the daily climatology (seasonal cycle). Results are not sensitive to how the anomalies are defined. A hamming window is applied in both time and longitude in order to quantify phase speeds and zonal wavenumbers over the AtlanticNA region for individual seasons. Since the windowing inherently discards information on the edges of the domain, the AtlanticNA region is extended by 40° longitude to the east and west ($190^\circ - 30^\circ$ E) for the calculation of the spectra and the JAS season is extended to JJASO and the OND season to SONDJ. These extensions give weights of approximately $1/e$ at the edges of the original domains (with a maximum weight of 1 in the domain center), but results are qualitatively similar if the domains are not extended.

Blocking identification

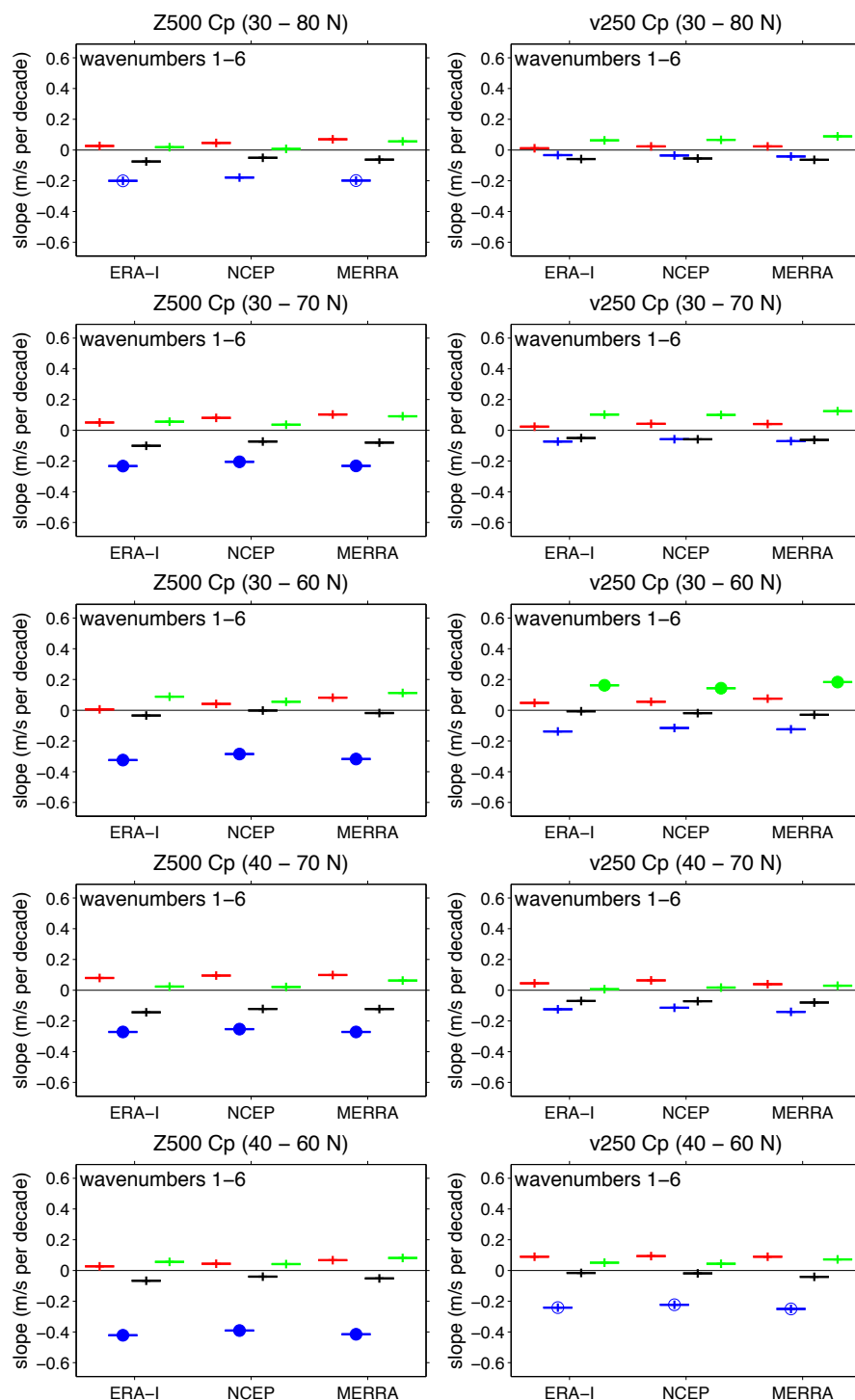
Blocking is diagnosed using the 1-dimensional blocking algorithm of [1] which identifies blocking regimes when the Z500 field exhibits a persistent (5 days or longer) reversal of its gradient. Blocked longitudes are grouped in time and space to form a single blocking regime and the position of a block is defined as the mean longitude of the blocking regime on its onset day. Note that this definition gives zonally-larger blocks the same weight as zonally-smaller blocks, so that the frequency is a measure of the number of days a block is *centered* at that longitude. All parameters and methods are identical to those of [1] except we smooth the eddy-kinetic energy field (used to define the seasonally varying storm track position) using a 7-day box-average filter to decrease computation time.

References

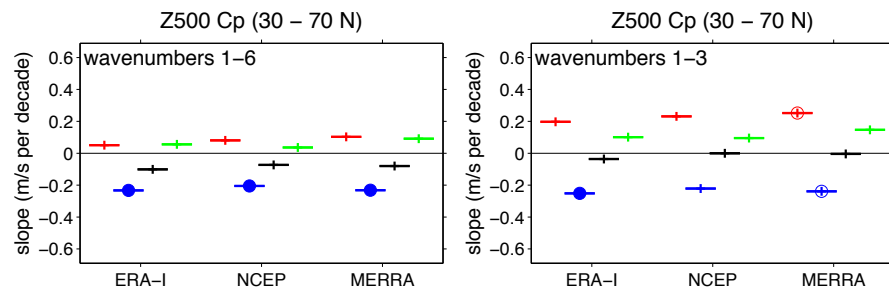
- [1] Elizabeth A. Barnes, Julia Slingo, and Tim Woollings. A methodology for the comparison of blocking climatologies across indices, models and climate scenarios. *Clim. Dynam.*, 38:2467–2481, 2012.
- [2] William Randel and Isaac Held. Phase speed spectra of transient eddy fluxes and critical layer absorption. *J. Atmos. Sci.*, 48, 1991.



Supplementary Figure 1: Seasonal AtlanticNA meridional extent as a function of the average latitude of the Z500 isopleth and the method used: (a,b) SeaMaxMin* and (c,d) DayMaxMin* for (a,c) JAS and (b,d) OND. Colored circles and dashed lines denote the maxima.



Supplementary Figure 2: Historical trends in the phase speed of waves with zonal wavenumbers 1-6 using the 250 meridional wind and 500 hPa geopotential height power spectra averaged over difference latitude bands. Plotted are values from 3 reanalyses between 1980-2011. Open circles denote trends that are statistically different from zero at 90% confidence and closed circles at 95%.



Supplementary Figure 3: Historical trends in the phase speed of waves with zonal wavenumbers 1-6 and 1-3 using the 500 hPa geopotential height power spectra. Plotted are values from 3 reanalyses between 1980-2011. Open circles denote trends that are statistically different from zero at 90% confidence and closed circles at 95%.